

Measurement of Hurst Exponents for Semiconductor Laser Phase Dynamics

Wing-Shun Lam,^{1,2} Will Ray,^{1,2} Parvez N. Guzdar,² and Rajarshi Roy^{1,2,3}

¹*Department of Physics, University of Maryland, College Park, Maryland 20742, USA*

²*IREAP, University of Maryland, College Park, Maryland 20742, USA*

³*IPST, University of Maryland, College Park, Maryland 20742, USA*

(Received 6 August 2004; published 3 January 2005)

The phase dynamics of a semiconductor laser with optical feedback is studied by construction of the Hilbert phase from its experimentally measured intensity time series. The Hurst exponent is evaluated for the phase fluctuations and grows from 0.5 to ~ 0.7 (indicating fractional Brownian motion) as the feedback strength is increased. A comparison with numerical computations based on a delay-differential equation model shows excellent agreement and reveals the relative roles of spontaneous emission noise and deterministic dynamics for different feedback strengths.

DOI: 10.1103/PhysRevLett.94.010602

PACS numbers: 05.40.Ca, 05.45.-a, 42.55.Px, 42.65.-k

The phase dynamics of nonlinear oscillators is relevant for systems ranging from biomedical engineering, atoms and molecules interacting with light, and charged particles in traps. Quite often, it is possible to experimentally determine the amplitude of dynamical variables, but the measurement of phase variables is much more elusive. Gabor's [1] introduction of the Hilbert transform to define an analytic signal from the amplitude of a dynamical variable made it possible to derive an associated phase. In recent years, such phase variables have been important in the study of nonlinear oscillator dynamics and synchronization [2,3]. When chaotic or noisy dynamics is displayed by such systems, the definition of a unique phase variable is often difficult due to the presence of multiple centers of rotation of the system trajectories.

In the context of the chaotic dynamics of the Lorentz model, Yalçinkaya and Lai [4] used an empirical mode decomposition (EMD) method [5] and the Hilbert transform to provide a uniquely defined phase variable and examine its dynamics. They showed that the Hurst exponent for the phase dynamics of this model chaotic system was about 0.74, representing persistent fractional Brownian motion of the phase [6].

In this Letter we experimentally estimate the Hurst exponent for measurements made on a semiconductor laser with optical feedback. We compare these results with computations on a delay-differential equation model of the system that includes the effects of stochastic noise and deterministic dynamics. A solitary semiconductor laser displays fluctuations of intensity about a steady state due to spontaneous emission noise that is inevitably present. When a fraction of the light output is fed back from an external reflector with a time delay, the system may exhibit a variety of dynamical phenomena [7]. In particular, when operated near threshold with moderate feedback strengths, the laser intensity output displays irregular power dropouts. If the laser is pumped further above threshold while subject to similar feedback conditions, the laser operates in the coherence collapse regime and is dominated by large amplitude chaotic oscillations

and the formation of many external cavity modes [8]. It is in the latter regime that we perform the measurements reported here.

In a previous study [9] we examined the formation of external cavity modes in this laser system. We identified mode formation through the observation of jumps of the Hilbert phase as calculated using a constant reference level, the average intensity of the laser. This procedure does not follow phase changes that may occur when the intensity displays nonstationary behavior, and is thus not suitable for a study of the scaling behavior of the phase dynamics, as measured by the Hurst exponent. We overcome this difficulty by defining a unique phase variable for the light intensity fluctuations through the combination of the EMD and Hilbert transform techniques and calculate the Hurst exponent for the system. Our results show that such measurements provide clear evidence for a transition from ordinary Brownian motion to persistent fractional Brownian motion of the phase as the amount of optical feedback coupled to the semiconductor laser is progressively increased. These measurements quantitatively distinguish the relative influence of spontaneous emission noise and deterministic dynamics due to reflective time-delayed feedback.

In the experiment, a temperature controller is used to stabilize (to better than 0.01 K) a Fabry-Perot semiconductor laser (Sharp LT015MD). The light ($\lambda = 830$ nm) from the laser is reflected by a mirror placed at a distance of 45 cm from the anti-reflection-coated facet. A beam splitter directs light onto a photodetector (12 GHz bandwidth). The output of the photodetector is recorded by a digital oscilloscope with 100 ps resolution. The laser is pumped with a bias current of 71.6 mA, which is 1.25 times of the threshold current of 57.2 mA. The amount of feedback coupled to the laser cavity is expressed through the effective external mirror reflectivity $R = \eta_c T^2$, which is characterized by the coupling efficiency η_c and the fraction of power T transmitted by a variable neutral density filter in the external cavity [10].

In Fig. 1(a), we show the real intensity time series $I^{(r)}(t)$ recorded for a feedback strength of $R = 6.7 \times 10^{-2}$. The Hilbert phase can be calculated for this time series by constructing the corresponding analytic signal $I(t) = I^{(r)}(t) + iI^{(i)}(t)$, where $I^{(i)} \equiv \pi^{-1}P \int_{-\infty}^{\infty} I^{(r)}(t') \times (t' - t)^{-1} dt'$ is the Hilbert transform of $I^{(r)}(t)$ and P is the principal value of the integral. Writing $I(t) = A(t)e^{i\phi_H(t)}$, where $A(t)$ is a real function, we obtain the Hilbert phase $\phi_H(t)$ of the real signal $I^{(r)}(t)$. The instantaneous Hilbert frequency $\omega(t) = d\phi_H(t)/dt$ can always be calculated from the Hilbert phase. This frequency quantifies the rate of rotation of $I(t)$ in the complex plane. However, $\omega(t)$ only bears physical significance as an oscillation when the analytic signal satisfies the conditions of proper rotation; namely, there is a preferred direction of rotation for $I(t)$ in the complex plane which can be defined with respect to a unique center. Amplitude variables of chaotic flows and noise-driven signals do not usually generate analytic signals with a proper structure of rotation [4,11].

The recently introduced EMD method [5] adaptively separates an arbitrary real time series into components, each possessing a proper rotation structure, according to the innate time scales of the dynamics. The EMD process is

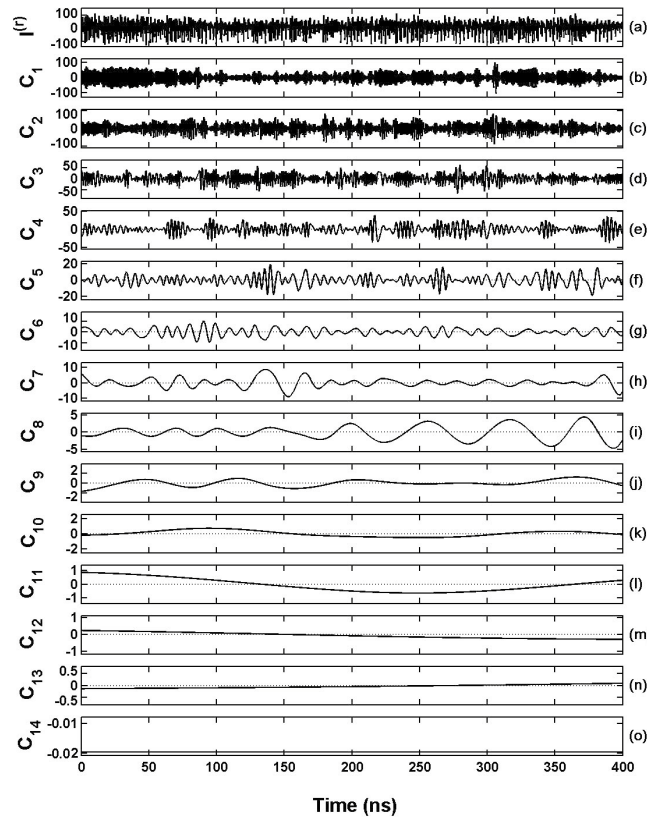


FIG. 1. (a) Intensity output of the semiconductor laser with $I = 71.6$ mA and $R = 6.7 \times 10^{-2}$. (b)–(o) 14 intrinsic mode functions for the time series of (a).

summarized as follows: (1) construct two smooth splines connecting all the maxima and minima, respectively, to get $I_{\max}^{(r)}(t)$ and $I_{\min}^{(r)}(t)$; (2) compute $\Delta I^{(r)}(t) \equiv I^{(r)}(t) - [I_{\max}^{(r)}(t) + I_{\min}^{(r)}(t)]/2$; (3) iterate (1) and (2) for $\Delta I^{(r)}(t)$ until the resulting signal corresponds to a proper rotation. Denote the resulting signal by $C_1(t)$, which is the first intrinsic mode; (4) take the difference $I_1^{(r)}(t) \equiv I^{(r)}(t) - C_1(t)$ and repeat (1) to (3) to obtain the second intrinsic mode $C_2(t)$; (5) continue the procedure, known as sifting, until the mode $C_M(t)$ shows no apparent variation.

By performing these steps, we have decomposed the original signal $I^{(r)}(t)$ into $\sum_{j=1}^M C_j(t)$, where $C_j(t)$ is the j th intrinsic mode function (IMF) which is defined as a function satisfying the following two conditions: (1) in the whole data set, the number of extrema and the number of zero crossings must either be equal or differ at most by one; and (2) at any point, the mean value of the envelope defined by the local maxima and the envelope defined by the local minima is zero. For the time series shown in Fig. 1(a), the EMD generates 14 IMFs, shown from Fig. 1(b) to Fig. 1(o). The properties of the IMFs ensure a proper structure of rotation for the corresponding analytic signals and allow a physically significant analysis of the Hilbert phase dynamics.

In Fig. 2(a), the 14 Hilbert phases $\phi_{H_i}(t)$ and the corresponding uniform phase increments calculated by $\langle \omega_i(t) \rangle t$ are plotted. The Hilbert phases (solid line) fluctuate about the dashed line representing the uniform increment. This is more clearly shown in Fig. 2(b), where $\delta\phi_{H_1}(t) \equiv [\phi_{H_1}(t) - \langle \omega_1(t) \rangle t]$ is portrayed for the intensity time series of Fig. 1(a) (thin line). We have focused on $\phi_{H_1}(t)$ since this phase variable represents the fastest observed time scales for the laser system. The 10 GHz sampling of laser intensity enables us to observe scaling of the phase fluctuations on the time scales involved in dynamical interactions between external cavity modes. The phase fluctuation of the first IMF is also shown for a time series recorded for a weaker feedback strength of $R = 7.2 \times 10^{-4}$ (thick line).

To examine the nature of the phase fluctuations, we calculate the Hurst exponent [6] of the time trace as follows: (1) choose a window with width w and obtain the absolute value of the phase difference $|\Delta\phi_{H_1}(t)| \equiv |\delta\phi_{H_1}(t+w) - \delta\phi_{H_1}(t)|$ by sliding the window from the beginning to the end of the time trace; (2) calculate $\langle |\Delta\phi_{H_1}(t)| \rangle$, which is the time average of the phase difference time series; (3) change the window size w and obtain the corresponding average value $\langle |\Delta\phi_{H_1}(t)| \rangle$; (4) plot $\log_{10}[\langle |\Delta\phi_{H_1}(t)| \rangle]$ versus $\log_{10}w$, if the plot distributes on a straight line, then the slope of the fit line is the Hurst exponent H of the time trace.

In Fig. 2(c), we plot $\log_{10}[\langle |\Delta\phi_{H_1}(t)| \rangle]$ versus $\log_{10}w$ for the phase fluctuations shown in Fig. 2(b). We find a scaling regime over about two decades of window width (from ~ 3 ns to ~ 150 ns). The Hilbert phase dynamics of the semiconductor laser system with a feedback of

$R = 7.2 \times 10^{-4}$ displays regular Brownian motion with a Hurst exponent $H = 0.50$. This is an indication that the fluctuations of the phase are dominated by spontaneous emission noise inherent to the laser. For a stronger feedback of $R = 6.7 \times 10^{-2}$, we measure $H = 0.71$. In this case, the dynamics portray a *persistent* fractional Brownian motion ($1 > H > 0.5$) of the phase and fluctuations are primarily influenced by the delayed feedback.

In order to obtain a clearer picture of how the phase dynamics are influenced by the feedback strength, we record 13 data sets with increasing feedback levels from $R = 0$ to $R = 0.18$, shown in Fig. 3. Our measurements in this coherence collapse regime ($R > 10^{-4}$) are characterized by rapid transitions between external cavity modes.

For the Hurst exponent analysis, we obtained eight intensity time traces for every feedback strength in the experiment. We could then calculate the average Hurst exponent and the standard deviation of the eight samples for each of the 13 feedback strengths [12]. The results are

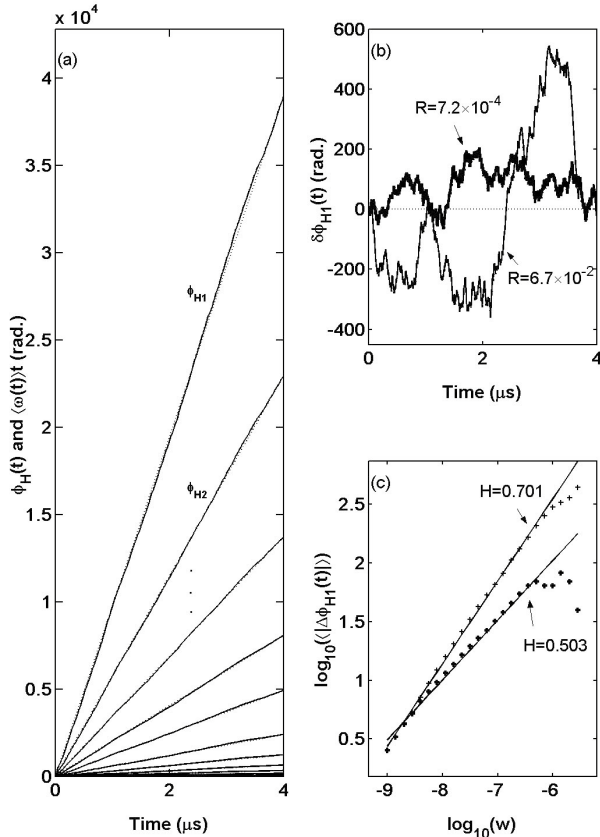


FIG. 2. (a) The Hilbert phases $\phi_{Hi}(t)$ of the IMFs in Fig. 1 (solid line) and the corresponding uniform phase increment $\langle \omega_i(t) \rangle t$ (dashed line), where $i = 1 \dots 14$, (b) the fluctuation of $\phi_{H1}(t)$ about the uniform phase increment $\langle \omega_1(t) \rangle t$ for (a) (thin line) and for a time series (not shown) with feedback strength $R = 7.2 \times 10^{-4}$ (thick line), and (c) the Hilbert phase dynamics is a persistent fractional Brownian motion with $H = 0.71$ for $R = 6.7 \times 10^{-2}$ and regular Brownian motion with $H = 0.50$ for $R = 7.2 \times 10^{-4}$.

displayed in Fig. 4 by the triangles. When the feedback strength changes from $R = 0$ to $R = 6.4 \times 10^{-3}$, the Hurst exponent stays close to 0.5 and the phase dynamics resemble regular Brownian motion. Spontaneous emission noise is the driving force of the intermode switching dynamics for this range of feedback. If the amount of feedback is increased past $R = 6.4 \times 10^{-3}$, the Hurst exponent exhibits a sharp increase towards 0.7 and levels off for feedback strengths greater than $R = 4.8 \times 10^{-2}$. In this regime, the phase dynamics is influenced by feedback and depends strongly on the history. Many external cavity modes now participate in the laser dynamics [7,13], and the Hurst exponent we compute now reflects an average of the scaling behavior of the phase dynamics for individual modes as well as contributions from deterministic global intermode interactions.

The experiment may be numerically modeled by integrating the Lang-Kobayashi equations [14] given below in a slightly different form [9]

$$\frac{dE}{dt} = \frac{1}{2}(1 + i\beta_c)G_{N,0}\sqrt{\frac{r_0}{r}}nE(t) + \kappa E(t - \tau)e^{-i\omega_0\tau} + F_E(t), \quad (1)$$

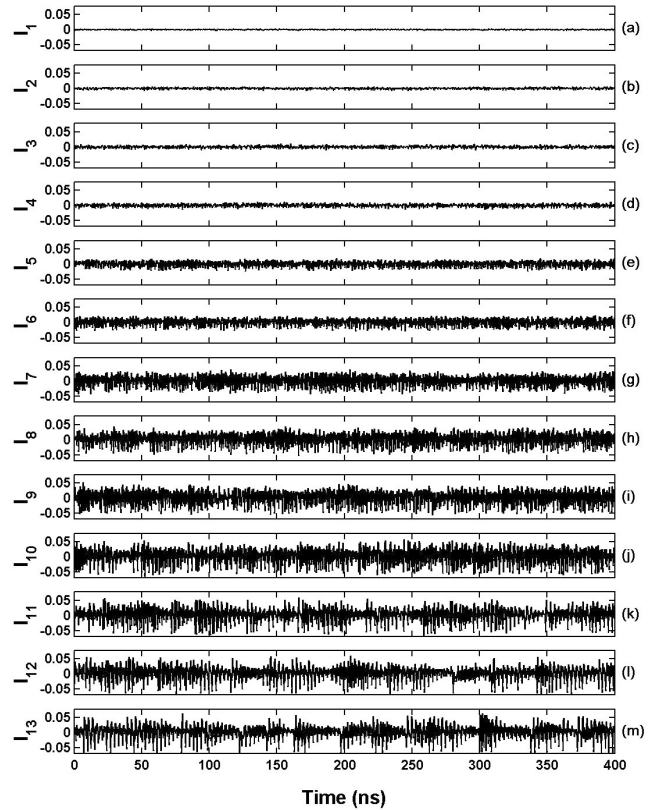


FIG. 3. (a)–(m) Experimental intensity time series with increasing feedback strength from $R = 0$ to $R = 0.18$. The pump current is set at 71.6 mA.

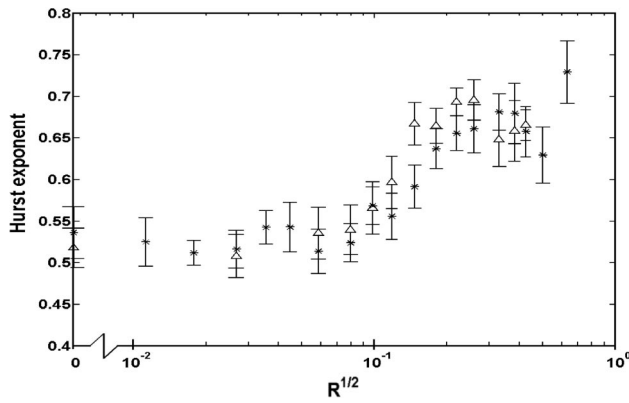


FIG. 4. The Hurst exponent with error bars for experimental measurements (triangles) and simulations (stars) for different feedback strengths. R shows the transition from regular ($H = 0.5$) to fractional ($H > 0.5$) Brownian motion.

$$\frac{dn}{dt} = (P_I - 1) \frac{N_{th}}{\tau_r} - \Gamma |E|^2 - n \left(\frac{1}{\tau_r} + G_{N,0} \sqrt{\frac{r_0}{r}} |E|^2 \right). \quad (2)$$

Here $E(t)$ is the complex field; $n(t) \equiv [N(t) - N_{th}]$ is the difference between the carrier number at arbitrary time and the threshold carrier number $N_{th} = 3.9 \times 10^8$; $\beta_c = 5$ is the linewidth enhancement factor; $G_{N,0} = 21400 \text{ s}^{-1}$ and $r_0 = 0.32$ are the respective differential gain and facet power reflectivity for a laser with an uncoated facet; $r = 0.1$ is the facet power reflectivity of a laser with an antireflection coating; $\tau = 3.0 \text{ ns}$ is the external cavity round-trip time; ω_0 is the solitary laser frequency; $F_E(t)$ is the Langevin noise term, with $\langle F_E(t) F_E(t')^* \rangle = R_{sp} \delta(t - t')$, where $R_{sp} = 10^{14} \text{ s}^{-1}$ is the spontaneous emission rate; $\tau_r = 1.1 \text{ ns}$ is the carrier recombination time and $\Gamma = 1.1 \text{ ps}^{-1}$ is the photon decay rate; $\kappa = (1 - r) \times (R/r)^{1/2} / \tau_{in}$ is the feedback rate, where $\tau_{in} = 3.9 \text{ ps}$ is the solitary laser pulse round trip time, and R the effective external mirror reflectivity used to quantify feedback levels in the experiment [9]. $P_I = 1.25$ is the ratio of pump and threshold currents. The equations are integrated with a time step of 0.5 ps for $41 \mu\text{s}$ (we neglect the first $1 \mu\text{s}$ for transients), low pass filtered and smoothed over intervals of 0.1 ns to simulate the digital oscilloscope electronics.

In Fig. 4 we also report the Hurst exponent versus the reflectivity from the simulations (stars), calculated for different R values matching the experiment and some additional cases. The computational results support the experimental conclusion that the dynamics of the Hilbert phase display ordinary Brownian motion for feedback strengths up to $R = 6.4 \times 10^{-3}$. Further increases in feedback show a transition to fractional Brownian motion and saturation of the Hurst exponent to $H \sim 0.7$, displaying a close match with experimental measurements.

We have experimentally confirmed for a real physical system the prediction by Yalçinkaya and Lai of persistent

Brownian motion for the most rapidly varying phase associated with a model chaotic system. In addition, we demonstrate that it is possible to distinguish between the influence of spontaneous emission noise and deterministic feedback on the dynamics of a semiconductor laser with optical feedback. The laser makes a transition from regular Brownian motion to persistent Brownian motion as the external mirror reflectivity is increased. The occurrence of this transition is quantified by measurements of the Hurst exponent for the phase dynamics computed from experimental and numerical time series for the laser intensity.

The authors thank N. Huang and M. Shlesinger for helpful discussions. We gratefully acknowledge support from the Office of Naval Research (Physics).

- [1] D. Gabor, J. IEE (London) **93**, 429 (1946); M. Born and E. Wolf, *Principles of Optics* (Cambridge University Press, Cambridge, England, 1999), 7th ed., pp. 557–562.
- [2] M. G. Rosenblum, A. S. Pikovsky, and J. Kurths, *Phys. Rev. Lett.* **76**, 1804 (1996).
- [3] A. S. Pikovsky, M. G. Rosenblum, and J. Kurths, *Synchronization: A Universal Concept in Nonlinear Sciences* (Cambridge University Press, Cambridge, England, 2001).
- [4] T. Yalçinkaya and Y. C. Lai, *Phys. Rev. Lett.* **79**, 3885 (1997).
- [5] N. E. Huang *et al.*, *Proc. R. Soc. London A* **454**, 903 (1998).
- [6] (a) H. E. Hurst, R. P. Black, and Y. M. Simaika, *Long-Term Storage: An Experimental Study* (Constable, London, 1965); (b) P. Addison, *Fractals and Chaos* (Inst. of Phys. Pub., London, 1997), Chap. 4.
- [7] J. Ohtsubo, *Prog. Opt.*, edited by E. Wolf (Elsevier, Amsterdam, 2002), Vol. 44, p. 1.
- [8] D. Lenstra, B. H. Verbeek, and A. J. Den Boef, *IEEE J. Quantum Electron.* **21**, 674 (1985).
- [9] W. S. Lam, P. N. Guzdar, and R. Roy, *Phys. Rev. E* **67**, 025604(R) (2003).
- [10] Simultaneous measurements of T and reduction of threshold current due to feedback $\Delta I_{th,fb}$ are fit to the logarithmic dependence of $\Delta I_{th,fb}$ on R for moderate levels of feedback. This procedure results in a best estimate of $\eta_c = 0.29$. K. Tatah and E. Garmire, *IEEE J. Quantum Electron.* **25**, 1800 (1989).
- [11] Y. C. Lai and N. Ye, *Int. J. Bifurcation Chaos Appl. Sci. Eng.* **13**, 1383 (2003).
- [12] The EMD process only approximates the conditions of proper rotation for each IMF. Details of EMD statistical analysis may be found in N. E. Huang *et al.*, *Proc. R. Soc. London A* **459**, 2317 (2003).
- [13] C. Masoller and N. B. Abraham, *Phys. Rev. A* **57**, 1313 (1998).
- [14] R. Lang and K. Kobayashi, *IEEE J. Quantum Electron.* **16**, 347 (1980).